

Magnetism in fcc rhodium and palladium

V. L. Moruzzi and P. M. Marcus

IBM Thomas J. Watson Research Center, P.O. Box 218, Yorktown Heights, New York 10598

(Received 30 June 1988; revised manuscript received 14 September 1988)

First-principles total-energy band calculations using the fixed-spin-moment procedure are used to study the volume dependence of the magnetic behavior for fcc Rh and Pd. We calculate the total energy, the magnetic moment, and the spin-polarized l -decomposed electron occupancy from below the equilibrium volume to the free-atom limit, and show the magnetic susceptibility in the nonmagnetic range. We find that both metals are nonmagnetic at zero pressure, but undergo first-order transitions from nonmagnetic to magnetic behavior at expanded volumes. In both cases, the onset of magnetic behavior is accompanied by magnetic moments that exceed the Hund's-rule atomic limit. With increasing volume, we find a depletion of s and p states and a corresponding increase of d states with an approach to the $4d^9$ and $4d^{10}$ free-atom configurations for Rh and Pd, respectively.

I. INTRODUCTION

Since transition-metal free atoms have magnetic moments consistent with Hund's rule and atomic ground-state configurations, all condensed transition-metal systems must also exhibit magnetic behavior at sufficiently large volumes. For normally magnetic transition metals, the onset of magnetic behavior occurs at volumes below equilibrium, whereas, for normally nonmagnetic transition metals, the onset occurs at expanded volumes. It has been shown that all transition metals exhibit an onset of magnetic behavior at well-defined critical volumes, and that the resulting transitions can be second-order, first order, or composite made up of a combination of second-order and first-order transitions.¹ In all cases, the onset of magnetic behavior is singular. That is, the magnetic moment increases with increasing volume with an infinite slope at the onset of magnetic behavior. In general, the magnetic moment of a condensed transition metal is less than Hund's rule applied to atomic ground-state configurations, and approaches the limiting values from below. As we will show, Rh and Pd are exceptions with magnetic moments exceeding Hund's rule and approaching the limiting values from above.

The normally nonmagnetic $4d$ fcc elements, Rh and Pd, are isoelectronic to the magnetic $3d$ elements, Co and Ni. It is therefore reasonable to expect these $4d$ elements to be nearly magnetic, even though the Pd free atom is nonmagnetic with a $4d^{10}5s^0$ configuration, and even though both Rh and Pd are nonmagnetic at zero-pressure equilibrium volumes. Both metals exhibit large paramagnetic susceptibilities, with the Pd susceptibility approximately twice that of Rh. In addition, late $3d$ transition metal impurities lead to ferromagnetic behavior² in both Rh and Pd. This incipient magnetic behavior implies interesting volume-dependent magnetic properties.

The expectation that Rh and Pd are "almost" magnetic even at equilibrium volumes has led to considerable interest in their electronic structure. Augmented plane wave (APW) band calculations³ for Pd and KKR band calculations⁴ for both Rh and Pd yield typical fcc

density-of-states (DOS) with the Fermi energy, E_F , located immediately above the sharp leading peak for Pd and just below the same peak for Rh. A recent relativistic treatment shows⁵ that without spin-orbit coupling Pd becomes magnetic at a 5% lattice expansion; with spin-orbit coupling, a 10% lattice expansion is required.

In the present work, we use nonrelativistic augmented-spherical-wave (ASW) spin-polarized band calculations⁶ and the fixed-spin-moment procedure⁷ to study the volume dependence of the magnetic behavior for metallic Rh and Pd from below the equilibrium volume up to the free-atom limit. We show that the onset of magnetic behavior is first order, with initial moments exceeding the Hund's-rule free-atom limit and that the moments decrease and approach the free-atom values at large volumes. Thus we show that our calculations yield the expected limiting free-atom magnetic behavior as well as the correct equilibrium zero-pressure behavior.

II. SPIN-POLARIZED CALCULATIONS

In Figs. 1 and 2, we present our calculated total energies and magnetic moments as functions of the Wigner-Seitz radius, r_{WS} [or equivalently, as functions of the volume, $V = (4\pi/3)r_{WS}^3$]. The total energies are given relative to the total energy of the free atom, E_a . For Rh, we find a nonmagnetic solution up to 3.32 a.u., and magnetic onset at 3.25 a.u. For Pd, the nonmagnetic solution terminates at $r_{WS} = 3.10$ a.u., and we find an onset of magnetic behavior at $r_{WS} = 3.06$ a.u. The equilibrium lattice separations are indicated on the figures. Since we find equilibrium at 2.81 and 2.88 a.u., we see that magnetism occurs at 16% and 6% (in agreement with Ref. 5) lattice expansions for Rh and Pd, respectively.

As shown, the magnetic moments for both systems are discontinuous at the transition, and have only limited ranges of coexistence for nonmagnetic and magnetic behavior. As a consequence, the two systems undergo weak first-order transitions, and show only small discontinuities in the slopes of the energy versus volume curves.

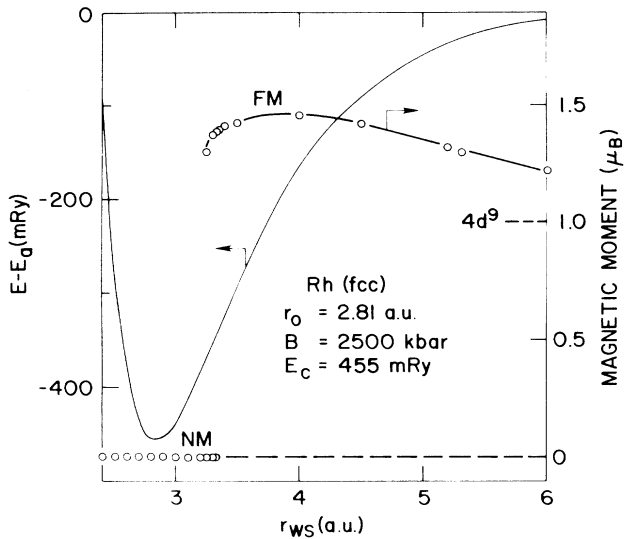


FIG. 1. Calculated magnetic moment and total energy as a function of r_{ws} for fcc Rh showing a weak first-order transition from a nonmagnetic (NM) to a ferromagnetic (FM) state. The termination of the NM state, and the beginning of the FM state define two critical points.

These discontinuities are not visible on the scale of Figs. 1 and 2.

For both Rh and Pd, we find that the initial magnetic moment (after the transition) exceeds the Hund's-rule free-atom limit, with values of 1.38 and $0.12 \mu_B$, respectively. In the large-volume limit, the total energies approach the free-atom values, and the magnetic moments approach values consistent with Hund's rule and $4d^9$ and

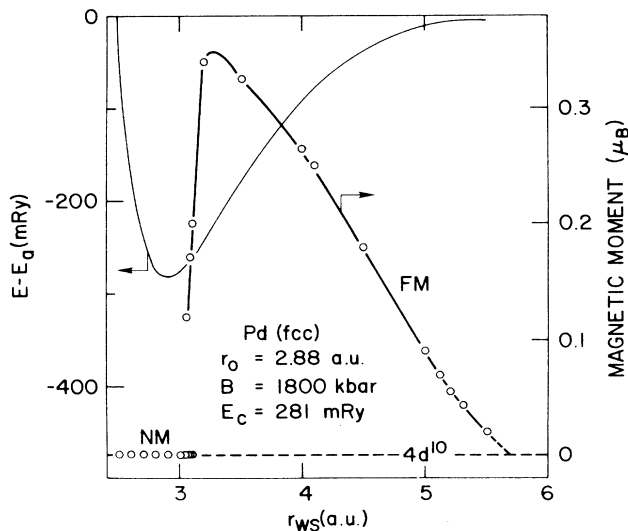


FIG. 2. Calculated magnetic moment and total energy as a function of r_{ws} for fcc Pd, showing a weak first-order transition from a nonmagnetic (NM) to a ferromagnetic (FM) state. The termination of the NM state, and the beginning of the FM state define two critical points.

$4d^{10}$ free-atom ground-state configurations from above, a behavior that is in contrast with most of the other transition metals.

A Stoner analysis based on the nonmagnetic DOS readily shows that the initial magnetic moments are a direct consequence of the integrated DOS from the Fermi energy to the lead peak. In Fig. 3 we show the DOS,⁴ for Rh and Pd at the equilibrium lattice separation. As shown, the Fermi energy for Rh lies well below the leading peak while the Fermi energy for Pd lies just above the peak. The relative difference between the initial magnetic moment values for the two systems is in good agreement with these integrated segments of the DOS.

In Figs. 4 and 5, we show the calculated volume dependence of the l -decomposed occupancy for the two systems up to $R_{ws} = 6$ a.u. The nonmagnetic solution extends up to a stability limit (the upper critical point) of 3.32 a.u. for Rh and 3.10 a.u. for Pd where the occupancies are not spin polarized. The magnetic solution begins at the lower critical point of 3.25 a.u. for Rh and 3.06 a.u. for Pd where spin-polarized occupancies are shown. In this region, the magnetic moment is the sum of the l -

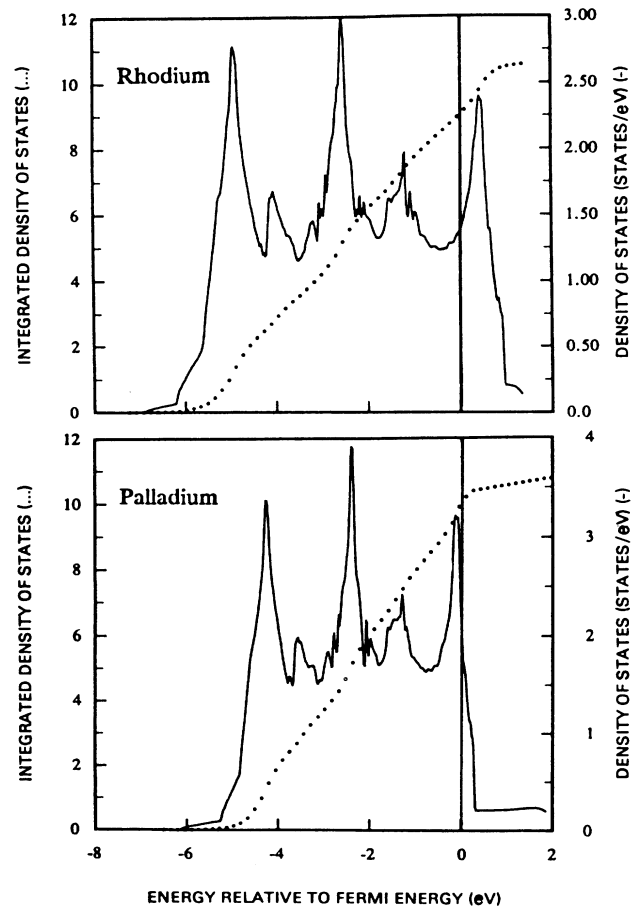


FIG. 3. Density of states at the equilibrium lattice separation for Rh and Pd taken from Ref. 4. The initial magnetic moments shown in Figs. 1 and 2 are a consequence of the integral from the Fermi energy to the leading peak.

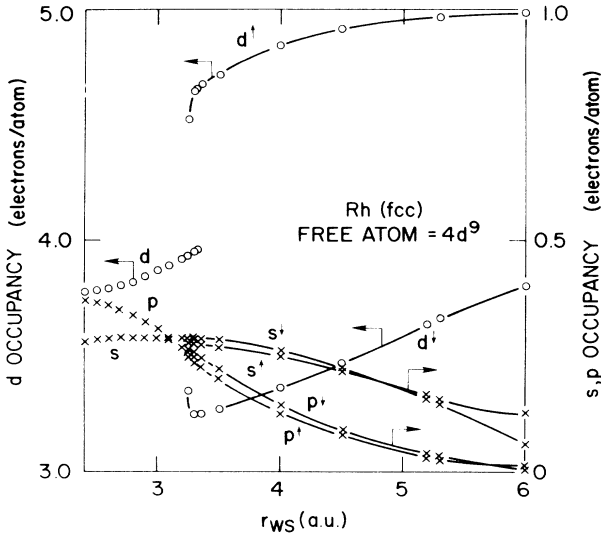


FIG. 4. Calculated spin-polarized electron occupancy as a function of r_{WS} for fcc Rh showing the discontinuity at the lower critical point where magnetic behavior begins.

decomposed occupancies. The discontinuity in the majority (up-spin) and minority (down-spin) d -band occupancy at the lower critical point reflects the singular nature of the transition. Our calculated s,p , and d spin-polarized occupancy shows that most of the magnetic moment can be accounted for by d -band polarization. For Rh, the s bands and the p bands are both polarized antiparallel to the d bands immediately above the transition, but the polarization changes sign at larger volumes. The large-volume limit implies $4d^5s^0$ and $4d^4s^0$ majority and minority band configurations and the experimental $4d^9$ composite ground-state configuration. For Pd, our calculations show that the s bands and p bands are only

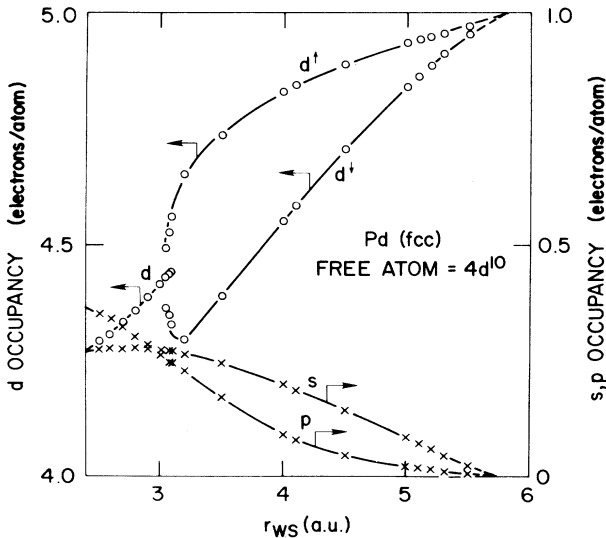


FIG. 5. Calculated spin-polarized electron occupancy as a function of r_{WS} for fcc Pd showing the discontinuity at the lower critical point where magnetic behavior begins.

slightly polarized (antiparallel to the d bands) and we show only the average occupancy. The differences between majority and minority band occupancy for the s band and p band are equal and relatively constant (≈ -0.01 electrons) throughout the range of magnetic behavior. Clearly, the large-volume limit implies that both the majority and minority d bands are full and that the s,p bands are completely empty. Thus we find $4d^5s^0$ and $4d^5s^0$ majority and minority band configurations and the experimental $4d^{10}$ composite ground-state configuration.

Figures 4 and 5 show that, with increasing volume, electron transfer occurs from the s,p bands to the d bands. Calculated DOS show that the s,p bands are gradually pushed to higher energies (above the Fermi energy), and that a gap develops when the s,p bands no longer overlap with the (spin-split) d bands. Electron transfer continues until atomic configurations are reached (where the spin-split s,p bands finally separate). In the process, the individual bands become narrower. Figures 1, 2, 4, and 5 show that, even at volumes where the free-atom configuration is achieved and electron transfer ceases, the total energy still does not reach the free-atom value because the bands still have finite widths. The small changes in total energy at still larger volumes are a consequence of final band narrowing to discrete atomic levels.

III. MAGNETIC SUSCEPTIBILITY

All of the results described in this work are derived from analysis of calculated $E(M)$ curves and their derivatives. The magnetic field, H , required to maintain the system at a magnetic moment, M , is given by $H = \partial E / \partial M$. Stable solutions are defined by magnetic moments that required no field and therefore correspond to local minima in $E(M)$ curves (local maxima define unstable solutions). If a local minimum occurs at $M = 0$, the system has a nonmagnetic solution; if a local minimum occurs at a finite M value, the system has a magnetic solution. For any solution, the magnetic susceptibility, χ , is given by,

$$\chi = \partial M / \partial H = 1 / (\partial^2 E / \partial M^2).$$

Thus, the susceptibility at a given solution can be found from the curvature of the $E(M)$ curve at any volume (Wigner-Seitz radius). In the nonmagnetic range, the curvature is taken at $M = 0$. Since the Pauli paramagnetic susceptibility, χ_0 , is,

$$\chi_0 = \mu_B^2 N(E_F),$$

where $N(E_F)$ is the DOS at the Fermi energy for one spin, and μ_B is the Bohr magneton, the susceptibility enhancement ratio, χ / χ_0 , is,

$$\chi / \chi_0 = 1 / [\mu_B^2 N(E_F) \partial^2 E / \partial M^2].$$

We expect χ / χ_0 to approach unity at low volumes where the systems have free electron behavior, and to become singular at the termination of nonmagnetic behavior.

At a given volume in the nonmagnetic range, χ is determined by fitting our calculated $E(M)$ curves to a Landau expansion (in even powers of M), and extracting

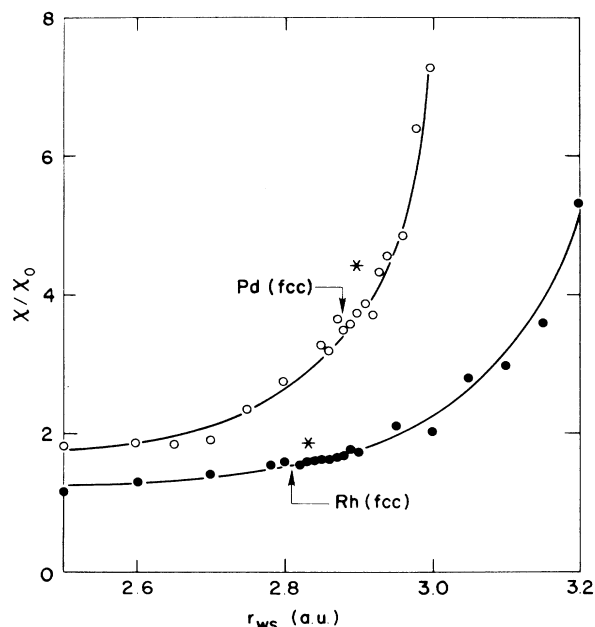


FIG. 6. Calculated susceptibility enhancement ratios as a function of r_{ws} for fcc Rh and Pd. Arrows indicate equilibrium, and * indicate points taken from Refs. 4 and 8.

the $M=0$ curvature. Figure 6 shows calculated χ/χ_0 as a function of r_{ws} for Rh and Pd. The volume dependence of χ/χ_0 depends upon details of the DOS through the volume dependence of the curvature of calculated $E(M)$ curves and $N(E_F)$. The apparent noise in the calculated points shown in the figure may be a reflection of these details.

Also shown in Fig. 6 are two points determined^{4,8} by using perturbation theory to find the response of each system (near the equilibrium volume) to a uniform external field. Our volume-dependent results are derived directly from spin-polarized calculations and $E(M)$ curves. The perturbation results are based on nonmag-

netic band calculations and involve an approximate determination of an exchange-correlation integral at the equilibrium volumes. We note the general agreement between the present and the perturbation results for both systems, and the large susceptibility for Pd.

IV. DISCUSSION

Theoretical ground-state properties are usually derived from an analysis of a fit of a calculated curve of total energy versus volume to a simple function. The function effectively smooths the calculated points and enables a better determination of the curvature used to determine the bulk modulus. Equilibrium Wigner-Seitz radii, bulk moduli, and cohesive energies derived from the position, curvature, and depth of the minimum in the total energy versus r_{ws} curves are indicated in Figs. 1 and 2. The listed cohesive energies contain an estimated zero-point lattice energy correction of 3 mRy for Rh and 2 mRy for Pd. Note that these results differ in detail from results⁹ of previous calculations. Our previous results are based on nonspin-polarized calculations which were fit to Morse functions over an extended volume range to facilitate a detailed thermal analysis. The present work is based on fixed-spin-moment spin-polarized calculations throughout the entire volume range, and differs from those of Ref. 9 by utilizing much fewer calculated points which are fit to a polynomial in the immediate vicinity of the energy minimum.

In summary, we have shown that our fixed-spin-moment spin-polarized results for Rh and Pd are in reasonable agreement with equilibrium ground-state properties, and that they approach the expected free-atom limit. Finally, we have calculated the susceptibility as a function of volume directly from our $E(M)$ curves, and compared these with previous results.

ACKNOWLEDGMENTS

We wish to thank P. C. Pattnaik and T. R. McGuire for helpful discussions and useful guidance.

¹V. L. Moruzzi, Phys. Rev. Lett. **57**, 2211 (1986); V. L. Moruzzi, P. M. Marcus, K. Schwarz, and P. Mohn, Phys. Rev. B **34**, 1784 (1986); V. L. Moruzzi, P. M. Marcus, and P. C. Pattnaik, *ibid.* **37**, 8003 (1988); V. L. Moruzzi, and P. M. Marcus, *ibid.* **38**, 1613 (1988); V. L. Moruzzi and P. M. Marcus, J. Appl. Phys. **64**, 5598 (1988).

²A. M. Clogston, B. T. Matthias, M. Peter, H. J. Williams, E. Corenzwit, and R. C. Sherwood, Phys. Rev. **125**, 541 (1962); R. M. Bozorth, H. J. Williams, and D. E. Walsh, *ibid.* **103**, 572 (1956).

³F. M. Mueller, A. J. Freeman, J. O. Dimmock, and A. M. Furdyna, Phys. Rev. B **1**, 4617 (1970).

⁴V. L. Moruzzi, J. F. Janak, and A. R. Williams, *Calculated Electronic Properties of Metals* (Pergamon, New York 1978).

⁵L. Fritsche, J. Noffke, and H. Eckardt, J. Phys. F **17**, 943 (1987).

⁶A. R. Williams, J. Kübler, and C. D. Gelatt, Jr., Phys. Rev. B **19**, 6094 (1979).

⁷A. R. Williams, V. L. Moruzzi, J. Kübler, and K. Schwarz, Bull. Am. Phys. Soc. **29**, 278 (1984); K. Schwarz and P. Mohn, J. Phys. F **14**, 1129 (1984).

⁸J. F. Janak, Phys. Rev. B **16**, 255 (1977).

⁹V. L. Moruzzi, J. F. Janak, and K. Schwarz, Phys. Rev. B **37**, 790 (1988).